POLITECNICO DI TORINO
Repository ISTITUZIONALE

Soft Error Reliability Prediction of SRAM-based FPGA Designs

Original
Soft Error Reliability Prediction of SRAM-based FPGA Designs / Vacca, E., Azimi, S., DE SIO, C., Portaluri, A., Rizzieri, D., Sterpone, L., Merodio Codinachs, D., Poivey, C.. - ELETTRONICO. - (2022), pp. 1-4. (IEEE Radiation and its Effects on Components and Systems 2022 Venice (ITA) 03-07 October 2022) [10.1109/RADECS55911.2022.10412546].

Availability:
This version is available at: 11583/2971147 since: 2022-10-13T12:58:58Z

Publisher:
IEEE

Published
DOI:10.1109/RADECS55911.2022.10412546

Terms of use:

This article is made available under terms and conditions as specified in the corresponding bibliographic description in the repository

Publisher copyright
IEEE postprint/Author's Accepted Manuscript

©2022 IEEE. Personal use of this material is permitted. Permission from IEEE must be obtained for all other uses, in any current or future media, including reprinting/republishing this material for advertising or promotional purposes, creating new collecting works, for resale or lists, or reuse of any copyrighted component of this work in other works.

(Article begins on next page)

06 September 2026

Available online at www.sciencedirect.com

ScienceDirect

Structural Integrity Procedia 00 (2022) 000–000

Structural Integrity Procedia

www.elsevier.com/locate/procedia

XIX ANIDIS Conference, Seismic Engineering in Italy

Influence of the Pier-abutment-deck interaction on the Seismic Response of Bridges Equipped with FPS

Elena Miceli[a]*, Luca Giordano[a]

[a]*Department of Structural, Geotechnical and Building Engineering (DISEG), Politecnico di Torino, Corso Duca degli Abruzzi 24, 10129, Turin, Italy*

Abstract

This work regards the analysis of the seismic response of bridges isolated with single concave friction pendulum devices, including or neglecting the presence of the rigid abutment. Two six degree-of-freedom models are considered for the two cases, in order to represent the response of the elastic reinforced concrete pier and of the infinitely rigid reinforced concrete deck. The behavior of the friction pendulum isolators accounts for the non-linear dependency of the friction coefficient on the sliding velocity. The comparison is carried out by including the aleatory uncertainty in the seismic input (i.e., accounting for different natural records with different characteristics) and by varying the modelling properties within a parametric analysis. Finally, by solving the equations of motion in nondimensional form, the difference between the two models are deepened in terms of influence of the seismic isolation.

© 2022 The Authors. Published by ELSEVIER B.V.
This is an open access article under the CC BY-NC-ND license (https://creativecommons.org/licenses/by-nc-nd/4.0)

Peer-review under responsibility of the scientific committee of the XIX ANIDIS Conference, Seismic Engineering in Italy
Keywords: seismic performance; seismic isolatio; friction pendulum bearings; non-dimensional equations.

1. Seismic isolation

Seismic isolation in case of bridges has the purpose of reducing the accelerations induced in the superstructures and consequently transmitted to the piers. Many works have focused on demonstrating the effectiveness of seismic isolation, as discussed in Constantinou et al. (1992), Kartoum et al. (1992) and Jangid (2008). For instance, the

* Corresponding author. Tel.: +39 0110905305.
E-mail address: elena.miceli@polito.it

2452-3216 © 2022 The Authors. Published by ELSEVIER B.V.
This is an open access article under the CC BY-NC-ND license (https://creativecommons.org/licenses/by-nc-nd/4.0)
Peer-review under responsibility of the scientific committee of the XIX ANIDIS Conference, Seismic Engineering in Italy

seismic performance of multi-span continuous deck bridges is studied in Kunde and Jangid (2006) with the adoption of simplified models to include the elastic behavior of the pier. A multi-span continuous deck bridge, isolated with elastomeric bearings, is investigated by Tongaonkar and Jangid (2003), with the purpose of analyzing the maximum displacement at the level of the device on the abutment. Among the widely spread bearings, the friction pendulum system (FPS) devices have the advantage of providing an isolation period independent from the mass of the deck, for their recentering ability as well as the capability to ensure high dissipation, as demonstrated in Su et al. (1989) and Wang et al. (1998). In particular, the concept of the existence of an optimum value for the friction coefficient of the FPS device able at minimizing the seismic response of the structure was first introduced by Jangid in Jangid (2000). In Castaldo and Amendola (2021a), the optimum friction coefficient is studied by changing many structural variables within a parametric analysis. Other parametric analyses have been elaborated in order to identify the influence on the seismic response of the design properties in case of isolated multi-span steel girder bridges, where FPS bearings were installed, as seen in Tubaldi et al. (2014) and Castaldo et al. (2018).

This work has the objective of studying the influence of neglecting or including the pier-abutment-deck interaction for bridges isolated with single concave friction pendulum devices (FPS). For this purpose, two six-degree-of-freedom (dofs) systems are modelled: one without the presence of the abutment and another considering its presence (i.e., single-column bent viaduct and multi-span continuous deck bridge respectively). Different problem parameters are varied within a parametric analysis and the uncertainty in the seismic input is included by means of a set of 30 natural ground motions. The equations of motion are solved for both the models in nondimensional form. The seismic response in terms of maximum normalized pier displacement is computed for both the structures and for all the seismic inputs. This has led to the computation of the optimum friction coefficient able to minimize the previously mentioned response and varying with the problem's parameters (i.e., deck and pier fundamental periods and mass ratio) allowing to compare the two systems.

2. Non dimensional form of the equations of motion

The two structures (i.e., single-column bent viaduct and multi-span continuous deck bridge) have been modelled by means of two six-degree-of-freedom (dof) systems, as shown in Fig. 1a and Fig. 1b respectively. In particular, 1 dof is used for the infinitely rigid reinforced concrete (RC) deck and 5 additional dofs are adopted for the lumped masses of RC pier, whose behavior is assumed elastic as discussed in Castaldo and Amendola (2021b). In addition, when the presence of the abutment is included, the latter is modelled as rigid and fixed.

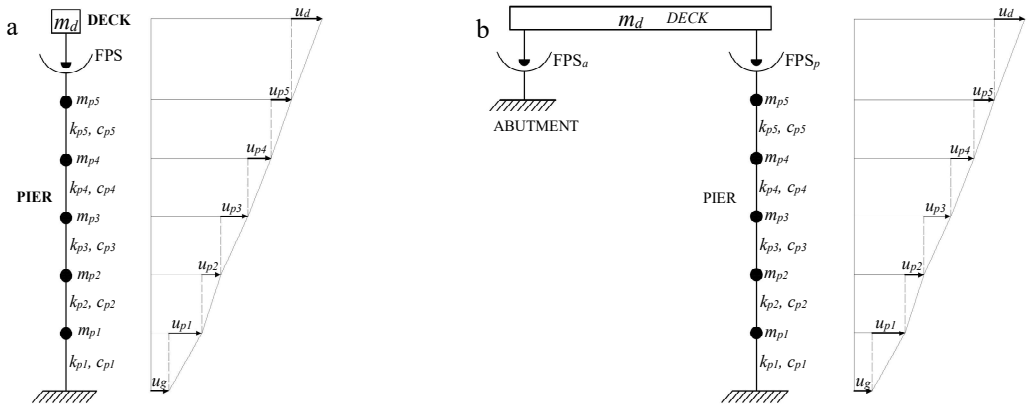

Fig. 1 Multi degree-of-freedom system for: (a) single-column bent viaduct (i.e., neglecting the presence of the rigid abutment); (b) multi-span continuous deck bridge (i.e., including the presence of the rigid abutment).

Regarding the case in which the abutment is modelled (Fig. 1b), the equation of motion under a horizontal seismic input are:

$$m_d\ddot{u}_d(t)+m_d\ddot{u}_{p5}(t)+m_d\ddot{u}_{p4}(t)+m_d\ddot{u}_{p3}(t)+m_d\ddot{u}_{p2}(t)+m_d\ddot{u}_{p1}(t)+c_d\dot{u}_d(t)+F_p(t)+F_a(t)=-m_d\ddot{u}_g(t) \tag{1a}$$

$$m_{p5}\ddot{u}_{p5}(t)+m_{p5}\ddot{u}_{p4}(t)+m_{p5}\ddot{u}_{p3}(t)+m_{p5}\ddot{u}_{p2}(t)+m_{p5}\ddot{u}_{p1}(t)-c_d\dot{u}_d(t)+c_{p5}\dot{u}_{p5}(t)+k_{p5}u_{p5}(t)-F_p(t)=-m_{p5}\ddot{u}_g(t) \tag{1b}$$

$$m_{p4}\ddot{u}_{p4}(t)+m_{p4}\ddot{u}_{p3}(t)+m_{p4}\ddot{u}_{p2}(t)+m_{p4}\ddot{u}_{p1}(t)-c_{p5}\dot{u}_{p5}(t)-k_{p5}u_{p5}(t)+c_{p4}\dot{u}_{p4}(t)+k_{p4}u_{p4}(t)=-m_{p4}\ddot{u}_g(t) \tag{1c}$$

$$m_{p3}\ddot{u}_{p3}(t)+m_{p3}\ddot{u}_{p2}(t)+m_{p3}\ddot{u}_{p1}(t)-c_{p4}\dot{u}_{p4}(t)-k_{p4}u_{p4}(t)+c_{p3}\dot{u}_{p3}(t)+k_{p3}u_{p3}(t)=-m_{p3}\ddot{u}_g(t) \tag{1d}$$

$$m_{p2}\ddot{u}_{p2}(t)+m_{p2}\ddot{u}_{p1}(t)-c_{p3}\dot{u}_{p3}(t)-k_{p3}u_{p3}(t)+c_{p2}\dot{u}_{p2}(t)+k_{p2}u_{p2}(t)=-m_{p2}\ddot{u}_g(t) \tag{1e}$$

$$m_{p1}\ddot{u}_{p1}(t)-c_{p2}\dot{u}_{p2}(t)-k_{p2}u_{p2}(t)+c_{p1}\dot{u}_{p1}(t)+k_{p1}u_{p1}(t)=-m_{p1}\ddot{u}_g(t) \tag{1f}$$

where u_d represents the displacement of the deck with respect to the pier, u_{pi} is the relative displacement of the i-th pier lumped mass with respect to the successive, m_d and m_{pi} are their respective masses, as well as c_d and c_{pi} are their respective viscous damping coefficients, k_{pi} stands for the stiffness of the pier lumped masses, t is the time, the dots indicate differentiation over time, $F_a(t)$ and $F_p(t)$ are the forces of the FPS isolators located, respectively, on top of the abutment and on the pier, computed as suggested by Zayas et al. (1990):

$$F_a(t)=\frac{m_d g}{2}\frac{1}{R_a}\left(u_d(t)+\sum_{i=1}^{5}u_{pi}\right)+\frac{m_d g}{2}\mu_a\left(\dot{u}_d+\sum_{i=1}^{5}\dot{u}_{pi}\right)\operatorname{sgn}\left(\dot{u}_d+\sum_{i=1}^{5}\dot{u}_{pi}\right) \tag{2a}$$

$$F_p(t)=\frac{m_d g}{2}\left[\frac{1}{R_p}u_d(t)+\mu_p(\dot{u}_d)\operatorname{sgn}(\dot{u}_d)\right] \tag{2b}$$

where $k_d=W/R=m_d g/R$ is the stiffness of the deck and is divided in two: half for the isolator on the abutment and half for the pier. The radii of curvature of the FPS devices on the abutment and on the pier, respectively, are R_a and R_p, μ is the sliding friction coefficient of the bearings, g is the gravity constant. It is noteworthy that the resistant forces of the bearings are given by the sum of an elastic component and a viscous component. In addition, the two forces differ only in terms of displacement since $F_a(t)$ depends on the displacement of the deck relative to the ground while $F_p(t)$ is function of the displacement of the deck with respect to the pier top. The fundamental period of the deck given by $T_d=2\pi\sqrt{m_d/k_d}=2\pi\sqrt{R/\mathrm{g}}$ only depends on the geometry of the isolator and it is independent from the deck mass (Zayas et al., 1990).

The sliding friction coefficient is given by a non-linear relationship with the sliding velocity as follows Mokha et al. (1990):

$$\mu(\dot{u}_d)=f_{\max}-(f_{\max}-f_{\min})\cdot\exp(-\alpha|\dot{u}_d|) \tag{3}$$

where $f_{\max}$ and $f_{\min}$ are the sliding friction parameters at large and zero velocity, the parameter α governs the transition from low to large velocities. In this study, it is assumed α equal to 30 and $f_{\max}=3f_{\min}$.

To obtain the nondimensional expression of the equations of motion, an application of the Buckingham's Π-theorem is adopted Makris and Black (2003). A time scale and a length scale are introduce as, respectively, $1/\omega_d$ (where ω_d indicates the circular frequency of the isolation system) and a_0/ω_d^2 (where a_0 is an intensity measure for the seismic input). In particular, the former is used to pass from the time t to $\tau=t\omega_d$, implying that the ground motion input of equation (1) is given by $\ddot{u}_g(t)=a_0 l(t)=a_0\ell(\tau)$, where $l(t)$ is the seismic input time-history over time t, while $\ell(\tau)$ is the same information but in the new time τ; the latter is introduced to divide all the members of equations (1) for a_0/ω_d^2. Then, the nondimensional equations are given by:

$$\begin{aligned}&\ddot{\psi}_d(\tau)+\ddot{\psi}_{p5}(\tau)+\ddot{\psi}_{p4}(\tau)+\ddot{\psi}_{p3}(\tau)+\ddot{\psi}_{p2}(\tau)+\ddot{\psi}_{p1}(\tau)+2\xi_d\frac{\omega_d}{\omega_g}\dot{\psi}_d(\tau)+\left[\frac{1}{2}\frac{\omega_d^2}{\omega_g^2}\psi_d(\tau)+\frac{\mu_p(\dot{u}_d)g}{2a_0}\operatorname{sgn}(\dot{\psi}_d)\right]+\\&+\frac{1}{2}\frac{\omega_d^2}{\omega_g^2}\left(\psi_d(\tau)+\sum_{i=1}^{5}\psi_{pi}(\tau)\right)+\frac{g}{2a_0}\mu_a(\dot{u}_d+\sum_{i=1}^{5}\dot{u}_{pi})\left(\operatorname{sgn}\left(\dot{\psi}_d+\sum_{i=1}^{5}\dot{\psi}_{pi}\right)\right)=-\ell(\tau)\end{aligned} \tag{4a}$$

$$\lambda_{p5}\left[\ddot{\psi}_{p5}(\tau)+\ddot{\psi}_{p4}(\tau)+\ddot{\psi}_{p3}(\tau)+\ddot{\psi}_{p2}(\tau)+\ddot{\psi}_{p1}(\tau)\right]-2\xi_d\frac{\omega_d}{\omega_g}\dot{\psi}_d(\tau)+$$
$$2\xi_{p5}\frac{\omega_{p5}}{\omega_g}\lambda_{p5}\dot{\psi}_{p5}(\tau)+\lambda_{p5}\frac{\omega_{p5}^2}{\omega_g^2}\psi_{p5}(\tau)-\left[\frac{1}{2}\frac{\omega_d^2}{\omega_g^2}\psi_d(\tau)+\frac{\mu_p(\dot{\psi}_d)g}{2a_0}\operatorname{sgn}(\dot{\psi}_d)\right]=-\lambda_{p5}\ell(\tau) \tag{4b}$$

$$\lambda_{p4}\left[\ddot{\psi}_{p4}(\tau)+\ddot{\psi}_{p3}(\tau)+\ddot{\psi}_{p2}(\tau)+\ddot{\psi}_{p1}(\tau)\right]-2\xi_{p5}\frac{\omega_{p5}}{\omega_g}\lambda_{p5}\dot{\psi}_{p5}(\tau)+2\xi_{p4}\frac{\omega_{p4}}{\omega_g}\lambda_{p4}\dot{\psi}_{p4}(\tau)-\lambda_{p5}\frac{\omega_{p5}^2}{\omega_g^2}\psi_{p5}(\tau)+\lambda_{p4}\frac{\omega_{p4}^2}{\omega_g^2}\psi_{p4}(\tau)=-\lambda_{p4}\ell(\tau) \tag{4c}$$

$$\lambda_{p3}\left[\ddot{\psi}_{p3}(\tau)+\ddot{\psi}_{p2}(\tau)+\ddot{\psi}_{p1}(\tau)\right]-2\xi_{p4}\frac{\omega_{p4}}{\omega_g}\lambda_{p4}\dot{\psi}_{p4}(\tau)+2\xi_{p3}\frac{\omega_{p3}}{\omega_g}\lambda_{p3}\dot{\psi}_{p3}(\tau)-\lambda_{p4}\frac{\omega_{p4}^2}{\omega_g^2}\psi_{p4}(\tau)+\lambda_{p3}\frac{\omega_{p3}^2}{\omega_g^2}\psi_{p3}(\tau)=-\lambda_{p3}\ell(\tau) \tag{4d}$$

$$\lambda_{p2}\left[\ddot{\psi}_{p2}(\tau)+\ddot{\psi}_{p1}(\tau)\right]-2\xi_{p3}\frac{\omega_{p3}}{\omega_g}\lambda_{p3}\dot{\psi}_{p3}(\tau)+2\xi_{p2}\frac{\omega_{p2}}{\omega_g}\lambda_{p2}\dot{\psi}_{p2}(\tau)-\lambda_{p3}\frac{\omega_{p3}^2}{\omega_g^2}\psi_{p3}(\tau)+\lambda_{p2}\frac{\omega_{p2}^2}{\omega_g^2}\psi_{p2}(\tau)=-\lambda_{p2}\ell(\tau) \tag{4e}$$

$$\lambda_{p1}\ddot{\psi}_{p1}(\tau)-2\xi_{p2}\frac{\omega_{p2}}{\omega_g}\lambda_{p2}\dot{\psi}_{p2}(\tau)+2\xi_{p1}\frac{\omega_{p1}}{\omega_g}\lambda_{p1}\dot{\psi}_{p1}(\tau)-\lambda_{p2}\frac{\omega_{p2}^2}{\omega_g^2}\psi_{p2}(\tau)+\lambda_{p1}\frac{\omega_{p1}^2}{\omega_g^2}\psi_{p1}(\tau)=-\lambda_{p1}\ell(\tau) \tag{4f}$$

where $\psi_d=u_d\omega_d^2/a_0$ and $\psi_{pi}=u_{pi}\omega_d^2/a_0$ are the nondimensional expressions for the displacement of the deck and of the pier respectively, $\omega_d=\sqrt{k_d/m_d}$ and $\omega_{pi}=\sqrt{k_{pi}/m_{pi}}$ are the respective circular vibration frequencies, $\xi_d=c_d/2m_d\,\omega_d$ and $\xi_{pi}=c_{pi}/2m_{pi}\,\omega_{pi}$ are the respective damping factors and $\lambda=m_{pi}/m_d$ is the mass ratio of the i-th lumped mass (equal for all the lumped masses). Then, the expression (4) is in terms of the following non dimensional parameters:

$$\Pi_{\omega_p}=\frac{\omega_p}{\omega_d},\quad \Pi_{\omega_g}=\frac{\omega_d}{\omega_g},\quad \Pi_\lambda=\lambda_p,\quad \Pi_{\xi_d}=\xi_d,\Pi_{\xi_p}=\xi_{pi},\quad \Pi_\mu=\frac{\mu(\dot{\psi}_d)g}{a_0} \tag{5}$$

More precisely, to avoid the dependency of the nondimensional parameter Π_μ from the velocity, its expression is substituted by $\Pi_\mu^*=f_{\max}g/a_0$.

All the previous considerations are valid for the case of a single-column bent viaduct (Fig. 1a). The only difference is that the term $F_a(t)$ is not present in both equations (1) and (4) since the abutment is not modelled.

3. Parametric analysis

In the following, the assumptions and considerations regarding the parametric analysis (valid, without distinction, for the two models) are presented.

Starting with the structural properties, the pier period T_p varies from 0.10s to 0.20s, the damping ratios are assumed equal to $\Pi_{\xi_d}=\xi_d=0\%$ and $\Pi_{\xi_p}=\xi_p=5\%$, the deck period T_d varies from 2s to 4s, the mass ratio varies in the range 0.1, 0.15, 0.2 and the normalized friction coefficient Π_μ^* ranges between 0 and 2.

For what concerns the seismic input, both the structures are subjected to 30 different seismic natural ground motions, selected from 19 different seismic events, coming from PEER, ITACA and ISESD databases. The main characteristics varies in the following ranges: the magnitude from 6.3 to 7.5, the peak ground acceleration from 0.13 to 0.82 g. the source-to-site distance from 13 km to 98 km. Regarding the seismic intensity a_0, also indicated as intensity measure in line with the Performance Based Earthquake Engineering (PBEE) approach Aslani and Miranda (2005), Porter (2003), is herein equal to the spectral pseudo-acceleration $S_A(T_d,\xi_d)$. In line with Ryan and Chopra (2004), the damping ratio ξ_d is set equal to zero, implying that the spectral pseudo-acceleration becomes only function of the deck fundamental period.

Starting from these assumptions, the equation of motions as shown in Equations (4) are numerically solved for each of the 30 natural ground motions and for both the two structural systems. The software that has been adopted is

Matlab Simulink, Math Works Inc (1997), and the algorithm used is the Runge-Kutta-Fehlberg integration algorithm. The output is in terms of maximum non dimensional displacement of the pier top, calculated as:

$$\psi_{u_p} = \frac{u_{p,\max}\omega_d^2}{a_0} = \frac{\left(\sum_{i=1}^{5} u_{p_i}\right)_{\max}\omega_d^2}{a_0} \tag{6}$$

The response parameter is subsequently probabilistically analyzed in order to obtain its statistics. In particular, the response is assumed to be lognormally distributed, in line with the results of Ryan and Chopra (1997) and Castaldo and Ripani (2016), having geometric mean $GM(D)$ and standard deviation $\beta(D)$ as follows:

$$GM(D) = \sqrt[N]{d_1 \cdot \ldots \cdot d_N} \tag{7a}$$

$$\beta(D) = \sqrt{\frac{\left(\ln d_1 - \ln\left[GM(D)\right]\right)^2 + .. + \left(\ln d_N - \ln\left[GM(D)\right]\right)^2}{N-1}} \tag{7b}$$

where d_i is the i-th sample realization of D, D is the response parameter herein assumed coincident with ψ_{u_p} and N represents the total number of samples (i.e., seismic inputs).

4. Comparison of the seismic response for the two structural systems

By solving the nondimensional equations of motion, the response in terms of nondimensional maximum displacement of the pier top is computed. Then, the geometric mean, calculated with respect to the results under the 30 natural ground motions, is calculated and shown in Fig.s 2-3. In particular, the two figures contains a comparison between the two structural systems as function of the deck periods T_d, the simplified nondimensional friction coefficient Π_μ^*, and for fixed values of T_p and m_p / m_d. For both the structural systems, the response decreases for lower values of the pier period and for larger values assumed by the deck period and the mass ratio. These results also suggest the existence of an optimal value for the friction coefficient able to minimize the seismic response of the substructure.

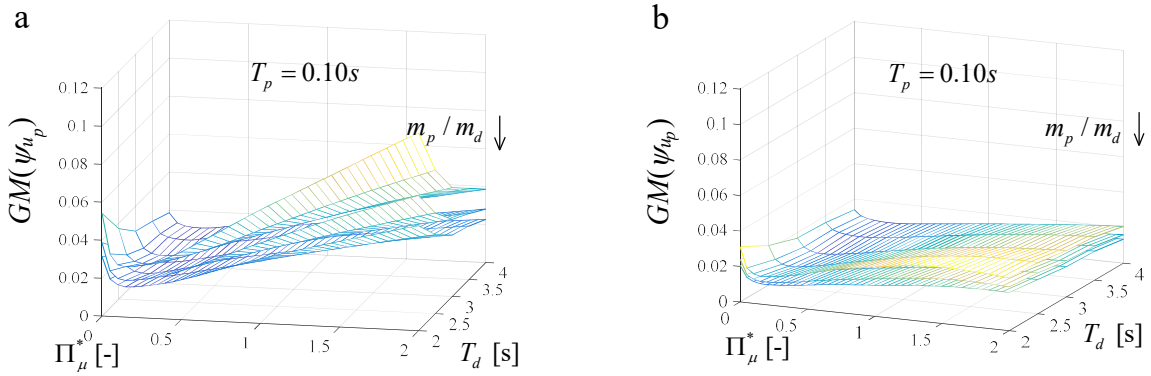

Fig. 2. Median value of the maximum normalized pier displacement as function of T_d and Π^*_μ, for m_p/m_d =0.1,0.15,0.3 and T_p =0.1s: (a) single-column bent viaduct; (b) multi-span continuous deck bridge.

Fig.s 4-5 contains the dispersion of the normalized maximum pier displacement. The dispersion is larger when the previously mentioned optimal value is reached and no other dependencies are recognized. Furthermore, for the case of the multi-span continuous deck bridge (i.e., modelling the pier-abutment-deck interaction) the dispersion is larger than the case of single-column bent viaduct.

It is noteworthy that the value of the optimal friction coefficient does not only depend on the variables of the problems (i.e., pier and deck fundamental periods and mass ratio), but it is also function of the structural system that is considered (i.e., if single-column bent viaduct or multi-span continuous deck bridge). Regarding this aspect, the sagging zones of the response in Fig.s 2-3 as function of Π^*_μ are more pronounced when the pier-deck-abutment interaction is neglected. This is explained by the larger sliding velocity of the bearing on top of the abutment than for the isolator on the pier.

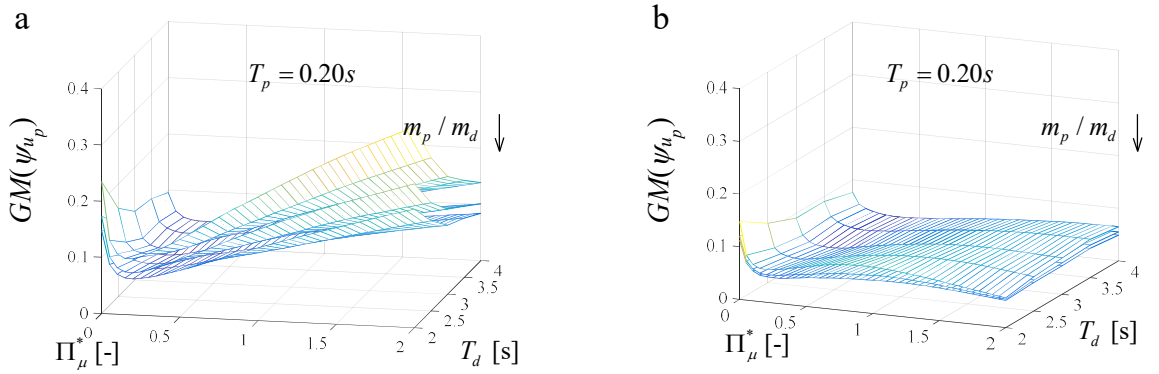

Fig. 3. Median value of the maximum normalized pier displacement as function of T_d and Π^*_μ, for m_p/m_d=0.1,0.15,0.3 and T_p=0.2s: (a) single-column bent viaduct; (b) multi span continuous deck bridge.

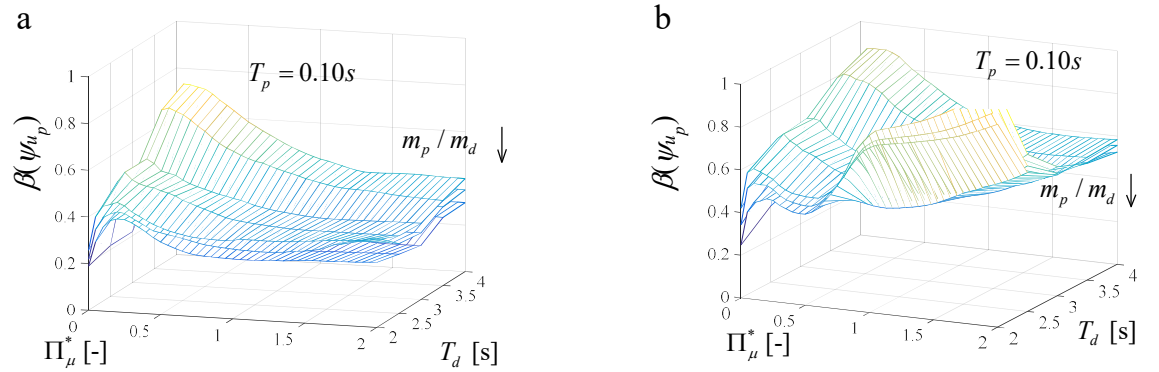

Fig. 4. Dispersion of the maximum normalized pier displacement as function of T_d and Π^*_μ, for m_p/m_d =0.1,0.15,0.3 and T_p =0.1s: (a) single-column bent viaduct; (b) multi-span continuous deck bridge.

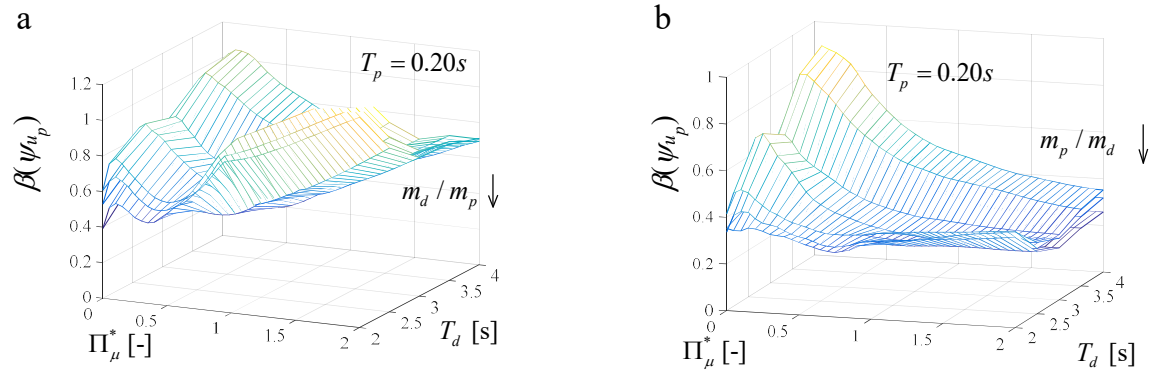

Fig. 5. Dispersion of the maximum normalized pier displacement as function of T_d and Π^*_μ, for m_p/m_d =0.1,0.15,0.3 and T_p =0.2s: (a) single-column bent viaduct; (b) multi span continuous deck bridge.

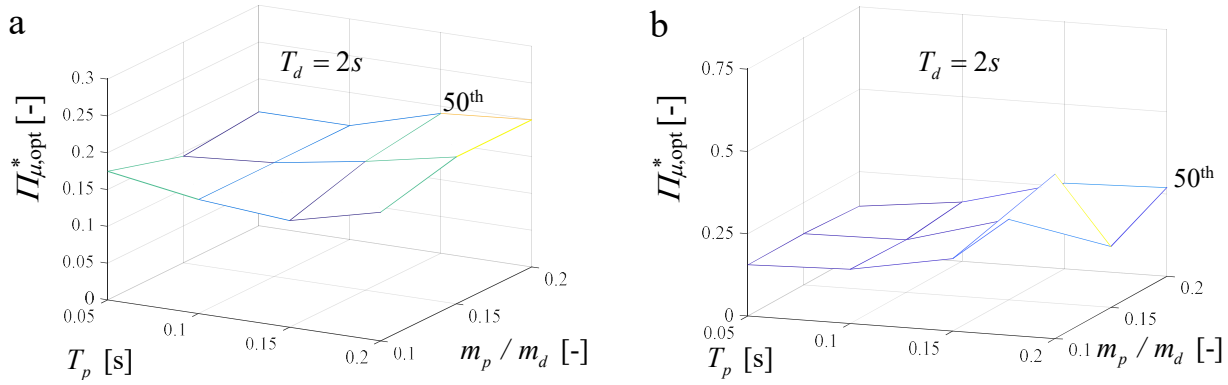

Fig. 6. Optimal friction coefficient as function of T_p, m_p/m_d and for T_d =2s: (a) single-column bent viaduct; (b) multi span continuous deck bridge.

.

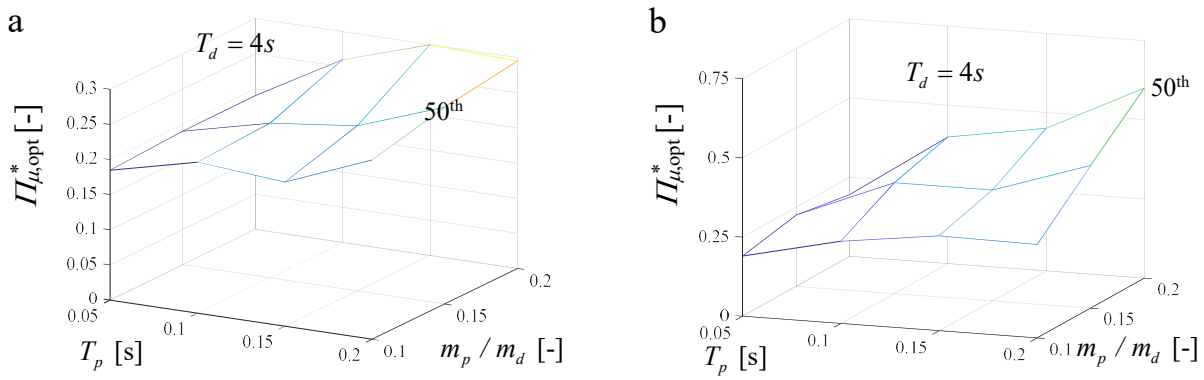

Fig. 7. Optimal friction coefficient as function of T_p, m_p/m_d and for T_d =4s: (a) single-column bent viaduct; (b) multi span continuous deck bridge.

The existence of an optimal friction coefficient has suggested to calculate its value as function of the other parameters involved in the problem. In Fig.s 6-7 this optimum is illustrated and indicated as $\Pi^*_{\mu,opt}$ for deck periods equal to 2s and 4s respectively. The interesting result is that when all the structural parameters (i.e., m_p / m_d, T_d and T_p) are larger, an higher optimum friction coefficient is required to minimize the pier response.

5. Conclusions

This study is focused on the evaluation of the seismic response of isolated bridges, comparing the case in which the pier-abutment-deck interaction is neglected or not. The first case is representative of a single-column bent viaduct and the second case regards a multi-span continuous deck bridge. The isolation is given by the presence of single concave friction pendulum devices placed on top of the pier (for the first case) and on top of both the pier and the abutment (for the other case). Two six-degree-of-freedom structural systems are modelled to solve the equations of motion, defined in a nondimensional form. Furthermore, different assumptions for the main structural parameters (i.e., pier and deck fundamental period, mass ratio and normalized friction coefficient) are included while the uncertainty in the seismic input is considered by means of 30 seismic inputs. The outputs in terms of geometric mean of the normalized maximum pier displacement indicate the existence of an optimum friction coefficient able to minimize the response of the substructure. This minimum of the response is more pronounced when the presence of

the abutment is neglected, since the bearing on the abutment (which is not present in the case of single-column bent viaduct) tends to slide faster than the one on the pier. The computation of the optimal friction coefficient as function of the other parameters involved (i.e., deck and pier fundamental periods and mass ratio) have shown how in general a larger optimal value is required when these parameters are larger and when the deck-abutment interaction is included.

References

Aslani, H., Miranda, E., 2005. Probability-based seismic response analysis. Engineering Structures 27(8), 1151-1163.

Castaldo, P., Ripani, M., 2016. Optimal design of friction pendulum system properties for isolated structures considering different soil conditions. Soil Dynamics and Earthquake Engineering 90, 74–87.

Castaldo, P., Ripani, M., Lo Piore, R., 2018. Influence of soil conditions on the optimal sliding friction coefficient for isolated bridges. Soil Dynamics and Earthquake Engineering 111, 131–148.

Castaldo, P., Amendola, G., 2021b. Optimal Sliding Friction Coefficients for Isolated Viaducts and Bridges. A Comparison Study. Structural Control and Health Monitoring 28(12).

Castaldo, P., Amendola, G., 2021a. Optimal DCFP bearing properties and seismic performance assessment in nondimensional form for isolated bridges. Earthquake Engineering and Structural Dynamics 50(9), 2442–2461.

Constantinou, M. C., Kartoum, A., Reinhorn, A. M., Bradford, P., 1992. Sliding isolation system for bridges: Experimental study. Earthquake Spectra 8(3), 321-344.

ISESD, Internet-Site for European Strong-Motion Data http://www.isesd.hi.is/ESD_Local/frameset.htm.

ITACA, Italian Accelerometric Archive http://itaca.mi.ingv.it/ItacaNet/itaca10_links.htm.

Jangid, R. S., 2000. Optimum frictional elements in sliding isolation systems. Computers and Structures 76(5), 651–661.

Jangid, R. S., 2008. Equivalent linear stochastic seismic response of isolated bridges. Journal of Sound and Vibration 309(3-5), 805-822.

Kartoum, A., Constantinou, M. C., Reinhorn, A. M., 1992. Sliding isolation system for bridges: Analytical study. Journal of Structural Engineering 8(3), 345-372.

Kunde, M. C., Jangid, R. S., 2006. Effects of pier and deck flexibility on the seismic response of isolated bridges. Journal of Bridge Engineering, 11(1), 109-121.

Makris, N., Black, C.J., 2003. Dimensional analysis of inelastic structures subjected to near fault ground motions. Technical report: EERC 2003/05, Berkeley: Earthquake Engineering Research Center, University of California.

Math Works Inc, 1997. MATLAB-High Performance Numeric Computation and Visualization Software. User's Guide. Natick (MA), USA.

Mokha, A., Constantinou, M. C., Reinhorn, A. M., 1990. Teflon Bearings in Base Isolation. I: Testing. Journal of Structural Engineering 116(2), 438-454.

PEER, Pacific Earthquake Engineering Research Center http://peer.berkeley.edu/.

Porter, K. A., 2003. An overview of PEER's performance-based earthquake engineering methodology, Proceedings of the 9th International Conference on Application of Statistics and Probability in Civil Engineering (ICASP9), San Francisco, California.

Ryan, K., Chopra, A., 2004. Estimation of Seismic Demands on Isolators Based on Nonlinear Analysis. Journal of Structural Engineering 130(3), 392-402.

Su, L., Ahmadi, G., Tadjbakhsh, I. G., 1989. Comparative study of base isolation systems. Journal of Engineering Mechanic 115(9), 1976–92.

Tongaonkar, N. P., Jangid, R. S., 2003. Seismic response of isolated bridges with soil–structure interaction. Soil Dynamics and Earthquake Engineering 23, 287–302.

Tubaldi, E., Ragni, L., Dall'Asta, A., 2014. Probabilistic seismic response assessment of linear systems equipped with nonlinear viscous dampers. Earthquake Engineering and Structural Dynamics 44 (1), 101-120.

Wang, Y. P., Chung, L. L., Liao, W.H., 1998. Seismic response analysis of bridges isolated with friction pendulum bearings. Earthquake Engineering and Structural Dynamics 27, 1069-1093.

Zayas, V., Low, S., Mahin, S., 1990. A simple pendulum technique for achieving seismic isolation. Earthquake Spectra 6(2), 317-333.